

## Research Article

## Microstructure Evolution of the Stainless Steel 316L Subjected to Different Routes of Equal Channel Angular Pressing

M. Askari Khan-Abadi, M.H. Farshidi\* and M.H. Moayed

Department of Materials Science and Metallurgical Engineering, Ferdowsi University of Mashhad, Mashhad, Iran

## ARTICLE INFO

*Article history:*

Received 12 October 2020

Reviewed 8 November 2020

Revised 26 November 2020

Accepted 2 January 2021

*Keywords:*

Severe plastic deformation

ECAP

Strain path

Dislocation density

Twinning

## ABSTRACT

During the past decades, equal channel angular pressing has risen as a promising severe plastic deformation process and it is applied for the grain refinement and strengthening of metallic materials. Although the application of this process to improve the characteristics of austenitic stainless steels has been studied to some extent, little studies have considered the effect of route of the ECAP on this matter. This study aims to study the evolution of microstructure and the increase of hardness of stainless steel 316L during processing by two different routes of this process. For this purpose, the alloy is processed at the deformation temperature of 310 °C using two different routes of A and B<sub>c</sub>. Afterwards, the microstructure evolution of the alloy is studied using the X-ray diffraction and the scanning electron microscopy. Results show that the applied ECAP procedure, irrespective of the applied route, causes a negligible occurrence of the phase transformation while it causes a widespread occurrence of twinning. This fact is related to the elevated temperature applied for the process. Also, the process causes a considerable increase in the hardness of the alloy mainly attributed to the occurrence of twinning.

© Shiraz University, Shiraz, Iran, 2021

### 1. Introduction

During the past decades, severe plastic deformation (SPD) has been developed as an attractive method for the grain refinement and the strengthening of metallic materials. Therefore, multiple processes have been developed to impose SPD on different shapes of materials like rods, tubes and sheets [1-3]. Among these processes, Equal Channel Angular Pressing (ECAP) is a favorable process because of its simplicity and its ability to impose a relatively homogenous strain. It is also notable that one of the attractive characteristics of the ECAP is its ability to impose a variable strain path on materials. As illustrated in Fig. 1, the path of strain

imposition can be changed after each pass of ECAP by applying different routes. For example, the position of specimen in each pass is similar to its position in the previous pass when using route A. This means that the strain path is constant in all passes when using this route. Despite this, when using route B<sub>c</sub>, the specimen is rotated for 90° by a constant twist direction after imposition of each pass that causes the variation of the strain path. Here, the strain path only repeats after imposition of four further passes. On the other hand, the alteration of the strain path can result in the alteration of the evolutions of microstructure and the increase of hardness [4-5]. For example, it is reported that the

\* Corresponding author  
 E-mail address: [farshidi@um.ac.ir](mailto:farshidi@um.ac.ir) (M.H. Farshidi)  
<https://doi.org/10.22099/ijmf.2021.38714.1169>

change of strain path may cause different microstructural effects like the reversal of micro-shear bands, the rapid generation of twins or the alteration of the hardening rate of the material [5-9]. However, despite different works focused on the effect of different ECAP routes on the characteristics of soft metallic materials like the aluminium alloys and the copper alloys, the effect of different ECAP routes on the characteristics of steels has not been studied [1-2]. This may be due to the considerable strength and the remarkable strain hardening of the steels that cause difficulties for the ECAP processing of these materials.

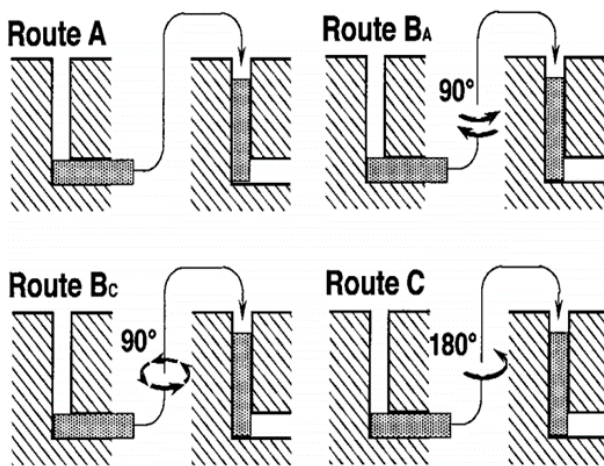


Fig. 1. Schematic illustration of different routes of the ECAP process [4].

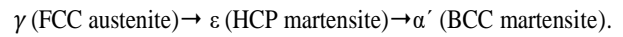
Austenitic steels are an important group of steels in which the austenite phase ( $\gamma$ ) is stabilized by the addition of different elements like Ni, Cu and Mn. To measure the stability of the austenite phase, the amounts of Ni-equivalent ( $Ni_e$ ) and Cr-equivalent ( $Cr_e$ ) are defined as below:

$$Ni_e = \% Ni + 30 (\% C + \% N) + 0.5 (\% Mn + \% Cu + \% Co) \quad (1)$$

$$Cr_e = \% Cr + 1.5 \% Si + \% Mo \quad (2)$$

Regarding the Schaeffler diagram shown in Fig. 2 [10], the  $Ni_e$  and the  $Cr_e$  characterize the stability of different phases like  $\gamma$  (FCC),  $\delta$  (BCC) and  $\alpha'$  (BCC). Notably, the stacking fault energy (SFE) of the  $\gamma$  phase of austenitic steels is remarkably low and therefore, the mobility of dislocations inside this phase is limited. Thus, the competing deformation mechanisms are activated during deformation of this phase. For further

explanation, it has been reported that the twinning occurs even during hot deformation of the austenitic steels [11-12]. Besides, cold deformation of these steels results in a transformation of austenite to martensite according to the below steps [13-14]:



It is also reported that the  $\gamma \rightarrow \alpha'$  martensitic transformation could occur directly. Nonetheless, it has been reported the volume fraction of  $\alpha'$  increases directly during the plastic deformation while the volume fraction of  $\epsilon$  goes to a maximum and then falls. This fact can recommend the indirect transformation of  $\gamma$  to  $\alpha'$  during plastic deformation [13].

Stainless steels 3XX (SS3XX) are an important group of austenitic steels developed to service in extremely corrosive environments. As an illustration, SS316L is widely used for manufacturing of different parts of the pharmaceutical equipment and the petrochemical industries. This alloy typically contains 16-18 wt.% Cr, 10-14 wt.% Ni, 2-3 wt.% Mo and less than 2 wt.% of Mn as main alloying elements while its carbon content is less than 0.03 wt.%. Regarding this chemical composition and the Schaeffler diagram shown in Fig. 2, one can see that the  $\gamma$  phase is metastable in this alloy. Therefore, plastic deformation of this alloy can result is not only the occurrence of twinning but also the occurrence of the martensitic transformation. These phenomena result in a remarkable strain hardening of this alloy that is well documented in previous works [14-16]. However, most of the previous works have applied a constant strain path for the plastic deformation of this alloy. For more illustration, while there are a few studies conducted on the ECAP processing of SS316L, most of these works have considered only one route ( $B_c$ ) of the process. Therefore, the effect of applying different routes for ECAP processing of this alloy should be investigated. Also, previous studies have mainly considered the imposition of SPD on this alloy at the cold deformation regime and the warm SPD of this alloy has remained less considered. Therefore, the warm SPD of SS316L could be the target of further studies.

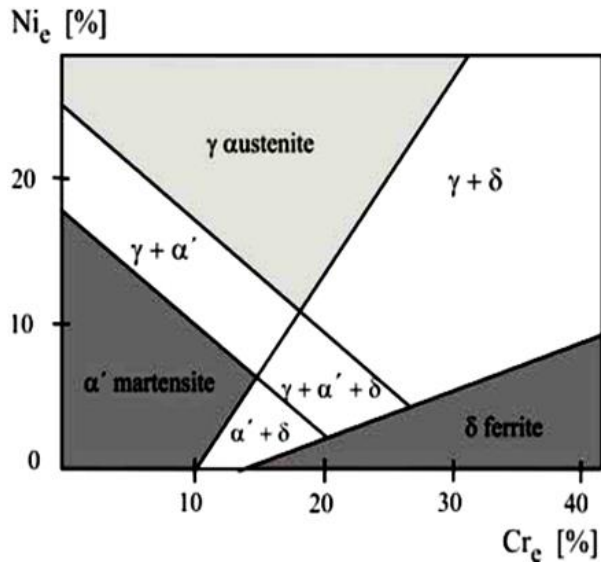


Fig. 2. Schaeffler diagram illustrating the stability of different phases of stainless steels [10].

This work aims to study the microstructure evolution and the hardness increase of SS316L during the warm SPD processing using two different routes of ECAP. For this purpose, the optical microscopy (OM), the scanning electron microscopy (SEM) and the X-ray diffraction (XRD) examinations are applied to characterize the evolution of microstructure while Vickers method is applied for measurement of the hardness.

## 2. Materials and Methods

An ECAP die for cylindrical specimens is manufactured with a channel angle of  $90^\circ$  as shown in Fig. 3. This die can be heated by four 250W electrical elements placed beside the main channel. The power of these elements causes heating of the die set from the room temperature to an elevated temperature of about

$310 \pm 30^\circ\text{C}$ . A rod of the SS316L with a diameter of 10 mm is supplied and it is cut to 60 mm long specimens. Table 1 illustrates the chemical composition of the supplied rod. After cutting, all of the specimens are subjected to an annealing step at  $1100^\circ\text{C}$  for 2h and then, they are quenched in water. Afterwards, the ECAP processing of specimens is accomplished using two different routes: A and B<sub>c</sub>. Hereafter, each specimen is called by a code which consists of the number of ECAP passes and the route of the process. For example, 4B<sub>c</sub> refers to the specimen ECAP processed for 4 passes using B<sub>c</sub> route. After ECAP processing, a 35 mm sample from the middle of each specimen is cut for the microstructural observations and the hardness measurements. Note that since the length of the initial specimen was 60 mm, one can expect that the imposed plastic deformation on this area of specimens is relatively homogenous.

XRD experiments are accomplished on the transversal plane of specimens using diffraction angles between  $40^\circ$  to  $90^\circ$ . The Williamson-Hall (WH) method is applied to estimate the dislocation density of specimens using XRD results. Details of this method have been explained in previous works [17-18]. OM and SEM samples are cut from the transversal plane of specimens and are subjected to different electrochemical etching procedures shown in table 2. Also, Vickers microhardness measurement is accomplished using an indentation load of 49 N along the centerline of the transversal plane of specimens. The measurement of hardness is repeated for at least three times to obtain confident results.

Table 1. Chemical composition of the supplied alloy

Fe	Cr	Ni	Mn	Mo	S	P	Cu	Si	C
Remain	16.4	10	1.7	2.1	0.018	0.03	0.6	0.5	0.024

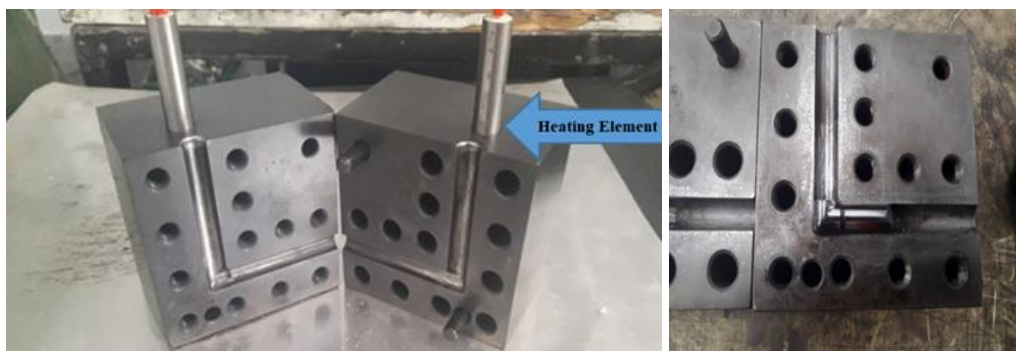


Fig. 3. The die set used for ECAP processing.

**Table 2.** Applied etching procedures and their targets

Etchant	Target	Procedure
HNO <sub>3</sub>	Austenite grain boundaries	8-12 sec. by 2v DC
2% Nital	General characteristics of microstructure	30 sec.
20% HCl in Methanol	Elongation of Austenite grains	15 sec.
40% HCl in Methanol	Appearance of twins	15 sec. by 4-6 v DC

### 3. Results and Discussions

Figure 4 illustrates the results of XRD experiments for different specimens. As can be seen here, three peaks related to the  $\gamma$  phase can be seen in the XRD profile of the annealed specimen. Also, the XRD profile of this specimen has a peak related to  $\delta$  phase. These peaks indicate the presence of  $\gamma$  and  $\delta$  phases inside the annealed specimen. As shown in Fig. 4, the peaks related to  $\gamma$  and  $\delta$  phases remain inside the alloy till imposition of 4 passes of ECAP while no evidence from the appearance of any peak related to the  $\epsilon$  or  $\alpha'$  phases is detected. This result indicates that the occurrence of the phase transformation through the used ECAP routes at the applied temperature is negligible. This result is in agreement with previous works on ECAP of this alloy. As an illustration, it is reported that the peaks of  $\delta$  phase persist through ECAP processing of the alloy at 353 K and 423 K using the B<sub>c</sub> route [20]. Besides, no evidence from the occurrence of martensitic transformation has been observed after ECAP processing was done through the B<sub>c</sub> route at different temperatures between 473 K to 673 K [17,19]. For more explanations, Equation 3 has been suggested for the temperature in which the half of the  $\gamma$  phase is transformed to the martensite after imposition of an engineering strain equal to 30% [21]:

$$M_{d30}(^{\circ}\text{C}) = 551 - 462(C + N) - 9.2Si - 8.1Mn - 13.7Cr - 29(Ni + Cu) - 18.5Mo - 68Nb - 1.42(Gs - 8) \quad (3)$$

Where Gs is the ASTM grain size number of steel. Considering the chemical composition of the alloy presented in table 1 and assuming the Gs equal to 5.5, the M<sub>d30</sub> temperature of the used steel is evaluated as -46 °C. Therefore, one can guess that the occurrence of martensitic transformation at the applied processing temperature should be negligible even through severe

straining by ECAP. Notably, the occurrence of martensitic transformation has been reported after imposition of an equivalent plastic strain of about 10 on the SS304L at a relatively elevated temperature [22]. The difference of the results of obtained by the present research on SS316L with that of SS304L can be attributed to different reasons. Firstly, considering the chemical composition of the SS304L, its M<sub>d30</sub> temperature is about 100°C above that of the similar temperature evaluated for SS316L. Secondly, the imposed plastic strain on the SS316L is relatively smaller than what is imposed on the SS304L [22]. As shown in Fig. 4, the increase of imposed ECAP passes results in broadening of the XRD peaks of the  $\gamma$  phase. A similar effect has been reported in previous works and it has been attributed to the increase of dislocation density of this phase [17, 20]. Table 3 shows the results of WH method for the estimation of the dislocation density of specimens. As can be seen here, the dislocation density of the alloy increases by the increase of ECAP pass number. In addition, one can see that the main increase of dislocation density occurs after the imposition of the first pass of ECAP while the imposition of further ECAP passes has less effect on the increase of dislocation density. Additionally, the magnitude of dislocation density of ECAP processed specimens are in agreement with the results of previous work on SPD of this alloy reported as  $1.3\text{-}7.2 \times 10^{14} \text{ 1/m}^2$  [17].

**Table 3.** Dislocation density of different specimens evaluated by WH method. The unit of the values is 1/m<sup>2</sup>

Pass No.	Route Bc	Route A
0		$7.8 \times 10^{13}$
1		$2.21 \times 10^{14}$
2	$4.08 \times 10^{14}$	$3.51 \times 10^{14}$
4	$5.23 \times 10^{14}$	$4.64 \times 10^{14}$

Figure 5 shows the microstructure of different specimens observed by OM and SEM. As shown in Fig. 5(a), equiaxed coarse grains of  $\gamma$  phase can be seen inside the microstructure of the annealed specimen. In addition,  $\delta$  phase islands can be traced inside  $\gamma$  grains as shown in Fig. 5(b). Additionally, the occurrence of twinning can be observed in microstructures of different specimens subjected to 1, 2 and 4 passes of ECAP using different routes. It is also notable that the aspect ratios of initial grains generally increase by the increase of ECAP pass number. However, one can see that the occurrence

of this effect is more severe after applying the route A in comparison with applying route B<sub>c</sub>. For instance, one can often trace grains with relatively small aspect ratios inside the microstructure of ECAP-B<sub>c</sub> processed specimens while all of the grains of ECAP-A processed specimens have great aspect ratios. This effect occurs because of the differences in the path of strain imposition between the applied ECAP routes. As discussed in previous studies, the strain path of route B<sub>c</sub> is reversible after every two passes. Therefore, while applying four passes of ECAP-B<sub>c</sub> theoretically causes no variation in the aspect ratio of a macroscopic element of the material, a macroscopic element of the material is severely elongated by the imposition of each pass of ECAP-A [23-25]. It is noteworthy that the limited increase of the aspect ratio of grains of the ECAP-B<sub>c</sub> processed specimens can be attributed to the difference between the macroscopic imposed strain and the strain imposed on each grain. This occurs because of the different alignment of grains towards the applied shear stress [24]. As shown in Fig. 5, a widespread occurrence of twinning can be seen in all ECAP-processed specimens irrespective of the applied ECAP routes. Note that the twin boundaries are characterized by two parallel lines inside the parent grains of the alloy. The widespread occurrence of twinning is in agreement with results of previous research conducted on ECAP processing of the SS316L. For instance, this effect is reported after the ECAP processing of this alloy at different deformation temperatures from near ambient to 400°C [17, 19-20, 27].

Figure 6 illustrates the variation of hardness inside ECAP processed specimens. As can be seen, the imposition of the first pass of ECAP causes a considerable increase of the hardness while the imposition of further ECAP passes causes a moderate one. Besides, the hardness increase through the ECAP-A is slightly smaller in comparison with what is seen through the ECAP-B<sub>c</sub>. Also, considering the calculated amount of the dislocation density shown in table 3, one can evaluate the hardening effect of the dislocation density increase as below [17]:

$$\Delta VHN = 3\alpha M G b \sqrt{\rho} \quad (4)$$

Where  $\alpha$  is a constant, M is the Tylor factor, G is the shear module of SS316L, b is the Burgers vector of this alloy and  $\rho$  is the dislocation density [17]. Considering  $\alpha$ , M, G and b equal to 0.25, 3.06, 77GPa and 0.25 nm,

one can see that the hardness increase of the alloy due to the increase of dislocation density through the imposition of 1, 2 and 4 passes of ECAP is respectively evaluated at about 28, 50 and 60 VHN. These amounts are considerably smaller than the whole increase of hardness through ECAP processing shown in Fig. 6. Therefore, it can be inferred that the main increase of hardness is related to the occurrence of twinning through ECAP processing. This result is in agreement with results of previous works on ECAP processing of this alloy [14-17, 19-20].

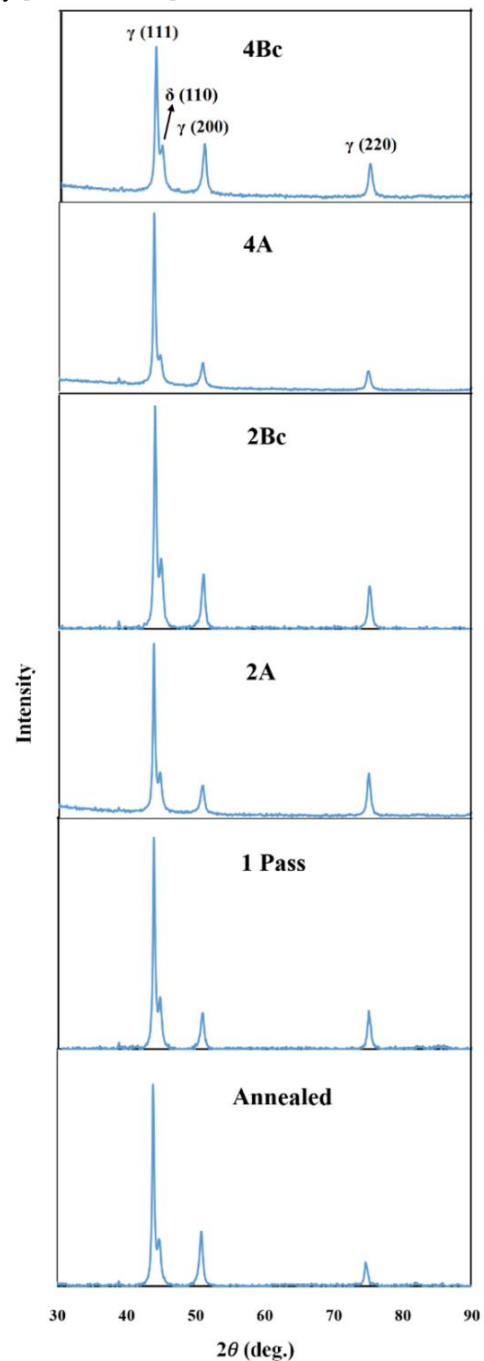


Fig. 4. XRD profile of different specimens.

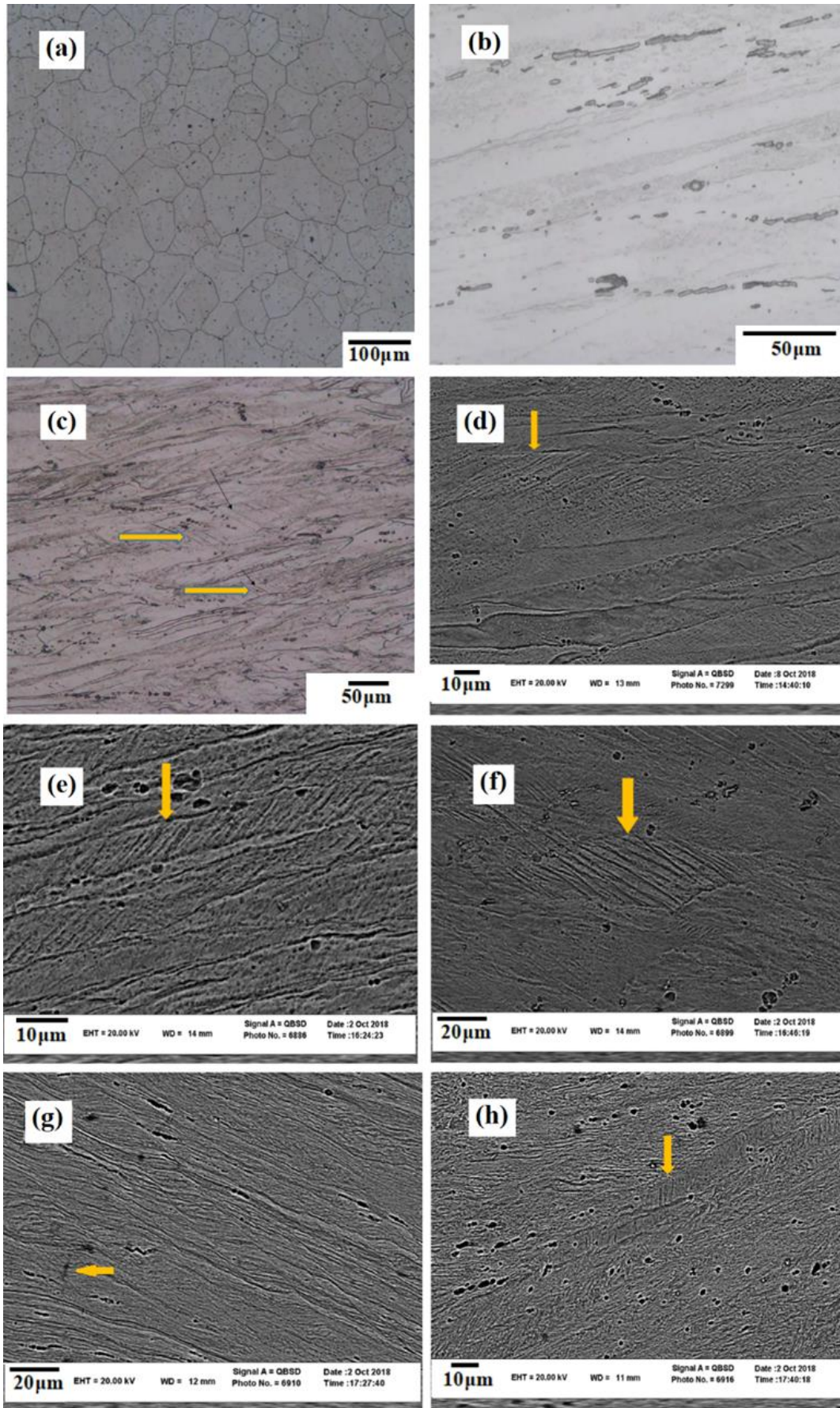


Fig. 5. Microstructure of: (a) and (b) the annealed, (c) and (d) 1 pass, (e) 2A, (f) 2Bc, (g) 4A, (h) 4Bc specimens.

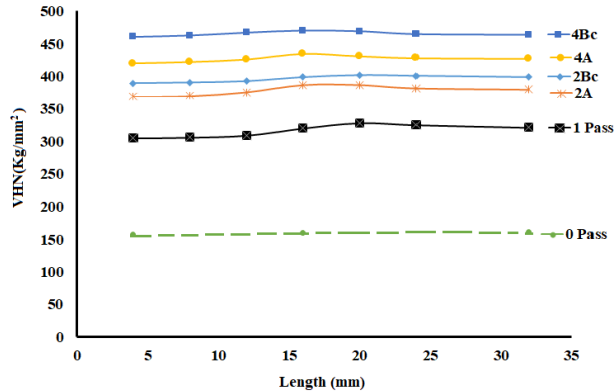


Fig. 6. Variation of hardness along the length of the centerline of different specimens.

#### 4. Conclusion

Considering the results of this study, the following conclusions can be made:

- 1- Irrespective of the applied route, ECAP processing of the SS316L at 310°C does not cause a considerable phase transformation but it does cause a widespread occurrence of twinning.
- 2- Using route A causes a severe increase in the aspect ratios of initial grains while this effect occurs moderately when using route B<sub>c</sub>.
- 3- Processing by ECAP causes an extensive increase in the hardness of the alloy. This effect is mainly attributed to the occurrence of twinning while the increase of the dislocation density has a limited effect on this subject.

#### 5. References

- [1] Y. Estrin, A. Vinogradov, Extreme grain refinement by severe plastic deformation: A wealth of challenging science, *Acta Materialia*, 61 (2013) 782-817.
- [2] E. Bagherpour, M. Reihanian, N. Pardis, R. Ebrahimi, T. G. Langdon, Ten Years of Severe Plastic Deformation (SPD) in Iran, part I: Equal-Channel Angular Pressing (ECAP), *Iranian Journal of Materials Forming*, 5 (1) (2018), 71-113.
- [3] E. Bagherpour, M. Reihanian, N. Pardis, R. Ebrahimi, N. Tsuji, Ten Years of Severe Plastic Deformation (SPD) in Iran, part II: Accumulative Roll Bonding (ARB), *Iranian Journal of Materials Forming*, 5(2) (2018) 1-109.
- [4] M. Furukawa, Z. Horita, M. Nemoto, T.G. Langdon, Processing of metals by equal-channel pressing, *Journal of Materials Science*, 36 (2001) 2835-2843.
- [5] A. Shan, I. Moon, H. Ko, J. Park, Direct observation of shear deformation during equal channel angular pressing of pure aluminum, *Scripta Materialia*, 41 (4) (1999) 353-357.
- [6] H. Miyamoto, T. Ikeda, T. Uenoya, A. Vinogradov, S. Hashimoto, Reversible nature of shear bands in copper single crystals subjected to iterative shear of ECAP in forward and reverse directions, *Materials Science and Engineering A*, 528 (2011) 2602-2609.
- [7] S. K. Mishra, S. M. Tiwari, A. M. Kumar, L. G. Hector, Effect of strain and strain Path on texture and twin development in austenitic steel with twinning-induced plasticity, *Metallurgical and Materials Transaction A*, 43A (2012) 1598-1609.
- [8] S. Seipp, M. F. X. Wagner, K. Hockauf, I. Schneider, L. W. Meyer, M. Hockauf, Microstructure, crystallographic texture and mechanical properties of the magnesium alloy AZ31B after different routes of thermo-mechanical processing, *International Journal of Plasticity*, 35 (2012) 155-166.
- [9] S. Mishra, K. Narasimhan, I. Samajdar, Deformation twinning in AISI 316L austenitic stainless steel: role of strain and strain path, *Materials Science and Technology*, 23 (9) (2007) 1118-1126.
- [10] I. Roth, M. Kubbeler, U. Krupp, H. J. Christ, C. P. Fritzen, Crack initiation and short crack growth in metastable austenitic stainless steel in the high cycle fatigue regime, *Procedia Engineering*, 2 (1) (2010) 941-948.
- [11] M. Calmunger, G. Chai, R. Eriksson, S. Johansson, J. J. Moverare, Characterization of Austenitic Stainless Steels Deformed at Elevated Temperature, *Metallurgical and Materials Transactions A*, 48 (2017) 4525-4538
- [12] X. Wang, D. Wang, J. Jin, J. Li, Effects of strain rates and twins evolution on dynamic recrystallization mechanisms of austenite stainless steel, *Materials Science & Engineering A*, 761 (2019) 138044.
- [13] M. J. Sohrabi, M. Naghizadeh, H. Mirzadeh, Deformation-induced martensite in austenitic stainless steels: A review, *Archives of Civil and Mechanical Engineering*, 20 (2020) 124.
- [14] J. Li, Y. Cao, B. Gao, Y. Li, Y. Zhu, Superior strength and ductility of 316L stainless steel with heterogeneous lamella structure, *Journal of Materials Science*, 53 (2018) 10442-10456.
- [15] F.Y. Dong, P. Zhang, J.C. Pang, D.M. Chen, K. Yang, Z.F. Zhang, Optimizing strength and ductility of austenitic stainless steels through equal-channel angular pressing and adding nitrogen element, *Materials Science & Engineering A*, 587 (2013) 185-191.
- [16] A. Jarvenpaa, M. Jaskari, A. Kisko, P. Karjalainen, Processing and Properties of Reversion-Treated Austenitic Stainless Steels, *Metals*, 10 (281) (2020) 1-43.
- [17] M. V. Karavaeva, M. M. Abramova, N. A. Enikeev, G. I. Raab, R. Z. Valiev, Superior Strength of Austenitic Steel Produced by Combined Processing, including Equal-

- Channel Angular Pressing and Rolling, *Metals* 6 (310) (2016) 1-14.
- [18] K. Ma, H. Wen, T. Hu, T. D. Topping, D. Isheim, D. N. Seidman, E. J. Lavermia, J. M. Schoenung, Mechanical behavior and strengthening mechanisms in ultrafine grain precipitation-strengthened aluminum alloy, *Acta Materialia* 62 (2014) 141-155.
- [19] S.V. Dobatkin, W. Skrotzki, O. V. Rybalchenko, V. F. Terentev, A. N. Belyakov, D.V. Prosvirmin, G. I. Raab, E. V. Zolotarev, Structural changes in metastable austenitic steel during equal channel angular pressing and subsequent cyclic deformation, *Materials Science and Engineering A*, 723 (2018) 141-147.
- [20] H. Ueno, K. Kakihata, Y. Kaneko, S. Hashimoto, A. Vinogradov, Nanostructurization assisted by twinning during equal channel angular pressing of metastable 316L stainless steel, *Journal of Materials Science*, 46 (2011) 4276-4283.
- [21] M. Soleimani, A. Kalhor, H. Mirzadeh, Transformation-induced plasticity (TRIP) in advanced steels: A review, *Materials Science and Engineering: A*, 795 (2020) 140023.
- [22] A. Zergani, H. Mirzadeh, R. Mahmudi, Evolutions of mechanical properties of AISI 304L stainless steel under shear loading, *Materials Science and Engineering: A*, 791(2020) 139667.
- [23] J. M. Garcia-Infanta, S. Swaminathan, A.P. Zhilyaev, F. Carreno, O. A. Ruano, T.R. Mc Nelley, Microstructural development during equal channel angular pressing of hypoeutectic Al-Si casting alloy by different processing routes, *Materials Science and Engineering A*, 485 (2008) 160-175.
- [24] R. Z. Valiev, T.G. Langdon, Principles of equal-channel angular pressing as a processing tool for grain refinement, *Progress in Materials Science*, 51 (7) (2006) 881-981.
- [25] M. Furukawa, Y. Iwahashi, Z. Horita, M. Nemoto, T. G. Langdon, The shearing characteristics associated with equal channel angular pressing, *Materials Science and Engineering A*, 257 (1998) 328-332.
- [26] H. Paul, T. Baudin, F. Brisset, The Effect of the strain path and the second phase particles on the microstructure and the texture evolution of the AA3104 alloy processed by ECAP, *Archives of Metallurgy and Materials*, 56 (2011) 245-261.
- [27] S. V. Dobatkin, V. F. Terent, W. Skrotzki, O. V. Rybalchenko, M. N. Pankova, D. V. Prosvirmin, E. V. Zolotarev, Structure and Fatigue Properties of 08Kh18N10T Steel after Equal Channel Angular Pressing and Heating, *Russian Metallurgy*, 2012, (11) (2012) 954-962.